OPEN ACCESS

Original research

Holdemanella biformis augments washed microbiota transplantation for the treatment of radiation enteritis

Weihong Wang,[1] You Yu,[1] Rui Wang,[1] Yaxue Wang,[1] Xiao Ding ,[2] Gaochen Lu,[1] Chen Lu,[1] Chenchen Liang,[1] Sheng Zhang,[1] Bo Yi,[3] Jianling Bai,[4] Lizhen Zhang,[5] Pan Li,[1] Quan Wen,[1] Bota Cui,[1] Faming Zhang [1]

► Additional supplemental material is published online only. To view, please visit the journal online (https://doi.org/10.1136/gutjnl-2025-335230).

[1]Department of Microbiota Medicine & Medical Center for Digestive Diseases, The Second Affiliated Hospital of Nanjing Medical University, Nanjing, Jiangsu, China
[2]CUHK Shenzhen Research Institute, The Chinese University of Hong Kong, Hong Kong, China
[3]The Second Abdominal Surgery Department, Jiangxi Cancer Hospital, Nanchang, Jiangxi, China
[4]Department of Biostatistics, Nanjing Medical University, Nanjing, Jiangsu, China
[5]Department of Radiation Oncology, The Second Affiliated Hospital of Nanjing Medical University, Nanjing, Jiangsu, China

Correspondence to
Professor Faming Zhang; fzhang@njmu.edu.cn and Dr Bota Cui; cuibota@njmu.edu.cn

WW, YY and RW contributed equally.

Received 5 March 2025
Accepted 26 August 2025
Published Online First 14 September 2025

To cite: Wang W, Yu Y, Wang R, *et al*. *Gut* 2026;**75**:289–301.

ABSTRACT

Background Current microbiome-based therapeutics face two prominent issues: the limited clinical efficacy of probiotics and the significant variability in the efficacy of microbiota transplantation across different diseases. Although washed microbiota transplantation (WMT) is a new faecal microbiota transplantation, a single therapeutic agent cannot be universally effective for multiple dysbiosis-related diseases.

Objective We introduced a new therapeutic concept, X-augmented WMT (X-auWMT), which combines a disease-specific beneficial microbe, 'X', with WMT to enhance its effectiveness. Our goal was to identify a candidate 'X' bacterium to augment WMT efficacy and examine the efficacy of X-auWMT in animal models of radiation enteritis (RE).

Design We conducted a prospective, non-randomised cohort study on a cohort of abdominal or pelvic cancer patients who developed RE after radiotherapy to identify a potential beneficial microbe. We used RE mouse models to evaluate the efficacy of X-auWMT compared with WMT. Multiomics analyses and experiments were undertaken to elucidate the underlying mechanisms.

Results WMT significantly alleviated multiple clinical symptoms in RE patients compared with routine treatments. We identified *Holdemanella biformis* as a candidate 'X' bacterium within the RE cohort and developed Hb-auWMT. Hb-auWMT significantly mitigated radiation-induced injury compared with WMT, exhibiting enhanced anti-apoptotic effects, improved maintenance of epithelial hypoxia, increased Treg cell levels and elevated butyrate and valerate levels in the RE mouse model. PPAR-γ is an essential pathway for the therapeutic efficacy of Hb-auWMT.

Conclusions This study overcomes the aforementioned recognised limitations with probiotics and microbiota transplantation and provides a new research paradigm in the concept of microbiome-based therapeutics.

WHAT IS ALREADY KNOWN ON THIS TOPIC

⇒ Radiation enteritis (RE) is a common complication of pelvic and abdominal radiotherapy, with gut microbiota dysbiosis affecting its development and progression.
⇒ Washed microbiota transplantation (WMT) has shown efficacy in treating RE in a case series.

WHAT THIS STUDY ADDS

⇒ WMT significantly enhanced clinical outcomes for RE patients compared with routine treatments in a cohort study.
⇒ *Holdemanella biformis* is a beneficial microbe in WMT for RE, absent in most patients but enriched in both responders and donors.
⇒ Hb-auWMT exhibited greater efficacy in the treatment of RE compared with WMT, associated with the elevated level of butyric acid and valeric acid.
⇒ Hb-auWMT activated epithelial PPAR-γ signalling to alleviate the RE and restore epithelial hypoxia in the colon.

HOW THIS STUDY MIGHT AFFECT RESEARCH, PRACTICE OR POLICY

⇒ Identifying key disease-linked bacteria and incorporating them into X-augmented WMT will expand research thoughts of microbiota-based therapies.

INTRODUCTION

Microbiome-based therapies have garnered global attention for advancing clinical practice. Probiotics and faecal microbiota transplantation (FMT) are widely used interventions for modulating gut microbiota and treating various diseases.[1] However, quality-controlled probiotic monotherapy often yields suboptimal clinical outcomes, while FMT, despite being highly effective for gut microbiota reconstruction, exhibits variable efficacy across different dysbiosis-related conditions.[2] Recent studies suggest that the survival and functional characteristics of specific bacterial strains significantly influence FMT outcomes.[3] These findings highlight the need for innovative microbiome-based therapies to address these limitations.

Gut microbiota dysbiosis varies across diseases and disease stages, with specific beneficial bacteria often absent or deficient during disease progression or in non-responders to FMT.[3] The new methods of FMT based on the automatic purification machine and the washing process were named as washed microbiota transplantation (WMT).[4] The WMT

procedure in the laboratory decreases over 73% of the FMT-related fever compared with the manual FMT procedure by washing out the pro-inflammatory agents in the faecal microbiota supernatant such as leukotriene B4, corticosterone and prostaglandin G2.[5] Building on this, we propose a novel therapeutic concept: augmenting WMT with disease-specific beneficial microbes (X-auWMT), where 'X' represents the targeted microbe. This approach aims to enhance therapeutic efficacy, though further research is needed to validate its principles and applications.

Despite the increasing use of radiotherapy in cancer treatment, radiation-induced adverse events (AEs) remain a significant challenge.[6 7] For instance, pelvic radiotherapy often causes acute or chronic radiation enteritis (RE).[8] Several high-quality studies on RE treatment have yielded negative results or demonstrated efficacy only for a single symptom, indicating that the available treatment options are limited.[9 10] The previous case series showed clinical improvement in three of five RE patients treated with WMT.[11] In this context, the present study aimed to evaluate the efficacy of WMT for RE, and identify specific beneficial bacteria associated with therapeutic response. We analysed faecal samples from abdominal or pelvic cancer patients with RE who underwent WMT, identifying *Holdemanella biformis* as a key taxon linked to anti-RE effects. This finding positions *H. biformis* as a promising candidate for augmenting WMT (Hb-auWMT) in RE treatment, with its efficacy further evaluated in animal models of RE.

MATERIAL AND METHODS

We conducted a prospective cohort study of abdominal or pelvic cancer patients who developed RE and were treated with either WMT or routine therapy. Faecal samples from patients and donors were analysed using shotgun metagenomic sequencing to identify key bacterial species. To evaluate the efficacy of Hb-auWMT, we employed radiation-induced RE mouse models. Intestinal barrier integrity, inflammation and gene expression were assessed through histopathology, immunohistochemistry, immunofluorescence, ELISA and RNA sequencing. Targeted metabolomics quantified short-chain fatty acids (SCFAs) in faecal samples, while immune cell populations in mouse models were analysed using flow cytometry and mass cytometry. Hypoxia in the colon was evaluated via PMDZ staining, and the retention of *H. biformis* in the colon was detected using FISH probes and FITC-D-Lysine fluorescence. The role of the PPAR-γ pathway in mediating Hb-auWMT's therapeutic effects was investigated through RNA-Seq, qRT-PCR and Western blot analysis, with the PPAR-γ antagonist GW9662 used to evaluate its significance. Detailed methodologies are provided in the online supplemental materials and methods.

RESULTS

The clinical therapeutic benefits of WMT in the RE cohort

The prospective, non-randomised cohort study design is presented in figure 1A. Among 233 screened patients with abdominal or pelvic cancers post-radiotherapy (online supplemental figure S1), 177 were diagnosed with RE and 120 completed the 3-month follow-up. To minimise baseline confounding, we performed propensity score matching at a 1:1 ratio between the WMT and non-WMT groups. After matching, each group comprised 51 patients, with balanced baseline characteristics, including age, gender, BMI and baseline Radiation Therapy Oncology Group (RTOG) scores (all standardised mean differences <0.1; online supplemental figure S2A). The WMT group received one course of WMT alongside routine therapies, while the non-WMT group received routine therapies alone. Baseline characteristics are detailed in table 1.

Given the absence of comparative data on WMT versus routine therapies for RE, we sought to determine whether WMT provided superior efficacy. The RTOG scale[12] was used to evaluate the severity of intestinal side effects from radiation therapy. We used the change in the RTOG scale compared with the baseline to calculate the clinical response and cure rates. The primary outcome, clinical response rate at week 12, was significantly higher in the WMT group (64.7% vs 27.5%, $p<0.001$, figure 1B). Because no cohort studies of FMT or WMT treating RE had been performed previously, no sample size calculation was conducted. Statistical power, calculated using Cramér's V (0.3737), was 0.9016, exceeding the 0.8 threshold, indicating reliable detection of significant differences. The response rates in the WMT group were also significantly higher at weeks 4 and 8 post-treatment (64.7% and 70.6%, respectively) compared with the non-WMT group (19.6% and 27.5%; both $p<0.001$, figure 1B). After adjusting for confounders (cancer stage, external beam radiotherapy details and duration of RE), WMT response rates remained significantly higher (adjusted $p<0.001$, figure 1B), with no multicollinearity issues (variance inflation factors <2.00). Clinical cure rates at weeks 8 and 12 were also higher in the WMT group (21.6% and 25.5%, respectively) versus the non-WMT group (7.8% and 7.8%, adjusted $p<0.05$, figure 1B). These results were consistent with the unmatched findings (online supplemental figure S2B), indicating the robustness of the matching approach.

Specific symptoms (diarrhoea, haematochezia, abdominal distension, abdominal pain, faecal incontinence) were evaluated using the Common Terminology Criteria for Adverse Events (CTCAE, version 5.0, figure 1C). Haematochezia and abdominal distension improved significantly in the WMT group compared with the non-WMT group at all time points ($p<0.05$, figure 1C), while diarrhoea improved at weeks 4 and 8 ($p<0.05$, figure 1C). MRI and endoscopy in the WMT group at week 12 showed reduced intestinal wall thickening, ulceration and exudation (figure 1D,E), whereas these improvements were not as pronounced in the non-WMT group (online supplemental figure S2C,D). Additionally, Vienna Proctoscopy Scores in the WMT group decreased significantly post-WMT ($p<0.0001$, figure 1F), indicating the injured mucosa recovered. AEs occurred in 2.08% of cases (3/144), all mild and resolved within 12 hours. No serious AEs were observed (table 2). Collectively, our clinical study demonstrates that WMT is more effective in treating RE compared with routine treatments. The global safety studies of FMT[13] and the safety evaluation of the present study both indicate that WMT is safe in treating RE.

H. biformis abundance increases in responders after WMT

To identify bacterial strains critical to clinical response, we selected 15 patients with complete faecal sample collection at baseline and 12 weeks post-WMT and their corresponding donors. Using shotgun metagenomic sequencing, these patients' microbiota alpha diversity showed an increasing trend (figure 1G, online supplemental figure S3A), while beta diversity shifted toward donor profiles (PEMANOVA, $p=0.01$, figure 1H). In the responder subgroup (patients achieving clinical response at week 12), alpha diversity significantly increased post-WMT ($p<0.05$, figure 1I). In contrast, non-responders did not demonstrate a significant improvement in alpha diversity post-WMT (online supplemental figure S3B,C). LefSe analysis

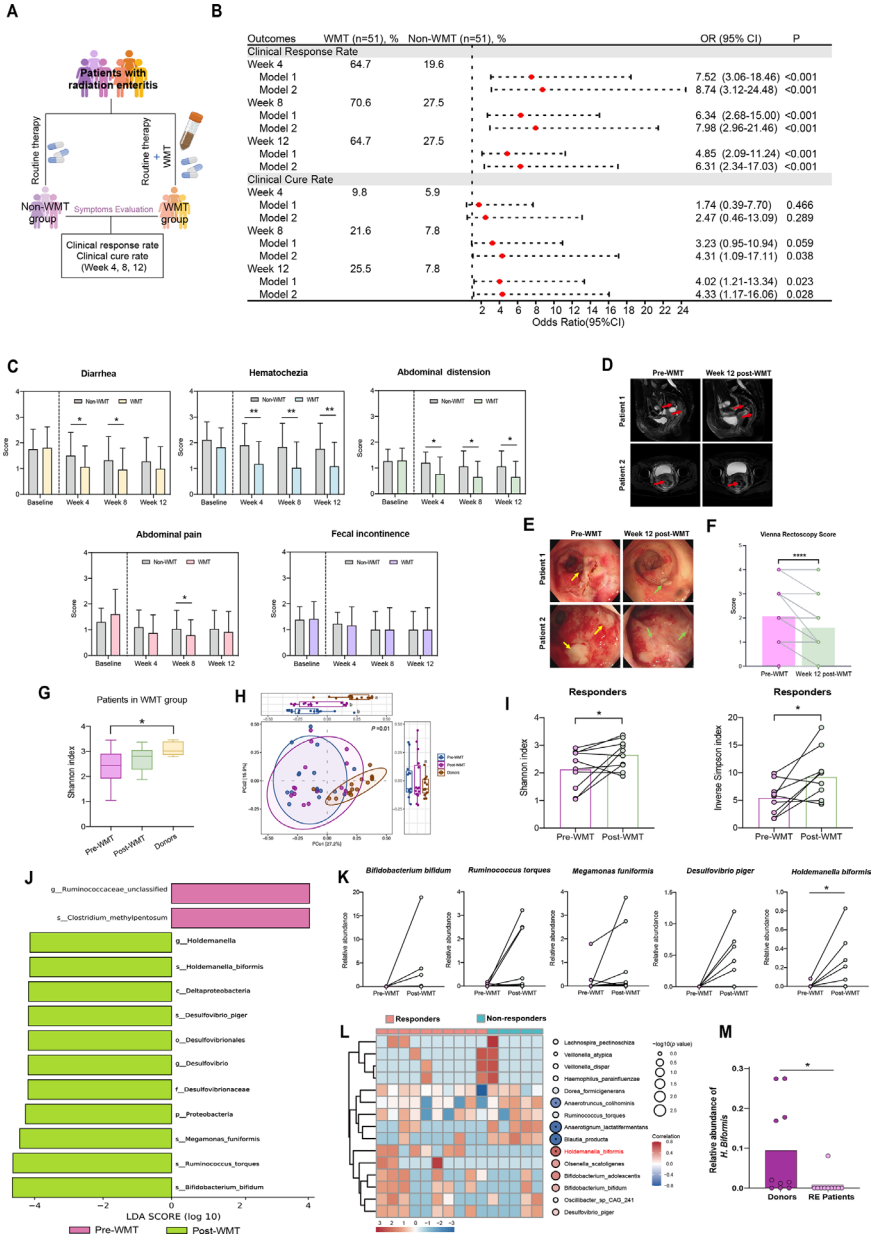

Figure 1 *Holdemanella biformis* is essential to the clinical efficacy of WMT for treating RE. (A) The design for the clinical trials. Symptoms were evaluated at weeks 4, 8 and 12 following treatments. (B) Comparison of the clinical response and cure rate in two groups at weeks 4, 8 and 12 following treatments. (C) Comparison of the CTCAE score for different symptoms in subgroups at weeks 4, 8 and 12 following treatments. Diarrhoea subgroup: WMT n=53, non-WMT n=49. Haematochezia subgroup: WMT n=30, non-WMT n=30. Abdominal distension subgroup: WMT n=17, non-WMT n=15. Abdominal pain subgroup: WMT n=34, non-WMT n=43. Faecal incontinence subgroup: WMT n=12, non-WMT n=13. (D) Representative MRI images of two patients with RE pre-WMT and week 12 post-WMT. The red arrow indicates the thickening of the intestinal wall and lumen. (E) Representative colonoscopic images of two patients with RE before WMT and week 12 post-WMT. The yellow arrow indicates the presence of colonic ulcers, and the green arrow highlights the alleviation of the ulcers. (F) Comparison of Vienna Proctoscopy Scores in patients of the WMT group (n=32) before and 12 weeks after WMT. (G) Comparison of the Shannon index among patients before and after WMT, and their donors (n=15). (H) PCoA analysis of faeces from patients who underwent WMT before and after treatment and their donors (n=15). Groups with statistically significant differences are indicated by distinct letters (eg, 'a' and 'b'), while groups sharing the same letter do not exhibit significant differences between them. (I) Comparison of the Shannon and inverse Simpson index among responders before and after WMT (n=10). (J) Histogram of the linear discriminant analysis (LDA) score between the responders before and after WMT treatment (LDA>4, n=10). (K) Comparison of the relative abundance of predominant bacterial species in responders before and after WMT treatment (n=10). (L) Heatmap analysis and Spearman's correlation analysis of differentially abundant in patients. The larger the circle, the smaller the p value; red indicates a positive correlation, while blue indicates a negative correlation. (M) Comparison of the relative abundance of *H. biformis* in donors and patients before WMT treatment (n=15). Data in B were compared using the adjusted binary logistic regression. Model 1: unadjusted. Model 2: adjusted for cancer stage, times of external beam radiotherapy, doses of external beam radiotherapy and duration of RE. Data in C were compared using the Mann-Whitney U test. Data in (F, I, K, M) were compared using the paired Student's t-test or Wilcoxon matched-pairs signed rank test. Data in (G) were presented as a boxplot, and p values were performed using an unpaired Student's t-test. Two-tailed *p<0.05, **p<0.01, ****p<0.0001. CTCAE, Common Terminology Criteria for Adverse Events; RE, radiation enteritis; RTOG, Radiation Therapy Oncology Group; WMT, washed microbiota transplantation.

Table 1 Baseline characteristics of the patients with RE

Characteristics	WMT group (n=51)	Non-WMT group (n=51)	P value
Gender			1.000
Male	7 (13.7)	7 (13.7)	
Female	44 (86.3)	44 (86.3)	
Age, years	60.2±10.6	61.0±10.2	0.705
BMI, kg/m^2	22.1±3.4	22.0±3.2	0.867
Location of cancer			0.882
Pelvic cavity	39 (76.5)	41 (80.4)	
Abdomen	11 (21.6)	9 (17.6)	
Prostate	1 (2.0)	1 (2.0)	
Cancer stage at radiation			0.099
I	6 (11.8)	2 (3.9)	
II	21 (41.2)	16 (31.4)	
III	20 (39.2)	22 (43.1)	
IV	4 (7.8)	11 (21.6)	
Duration of RE, months	8.0 (3.0–15.0)	7.0 (2.0–13.0)	0.221
Intracavitary radiation therapy	28 (54.9)	33 (64.7)	0.313
Total doses of irradiation, Gy	60.4 (48.6–78.4)	68.0 (50.0–76.6)	0.989
External beam radiotherapy			
Times, Fx	27.0 (25.0–28.0)	25.0 (25.0–27.0)	0.005
Dose, Gy	48.6 (46.8–50.6)	48.6 (45.0–50.0)	0.180
Diabetes	7 (13.7)	7 (13.7)	1.000
RTOG grade at baseline			0.735
1	8 (15.7)	7 (13.7)	
2	26 (51.0)	29 (56.9)	
3	14 (27.5)	14 (27.5)	
4	3 (5.9)	1 (2.0)	
Total amount of intestinal symptoms	3 (2-4)	3 (2-4)	0.994

Data are n (%), median (IQR) or mean±SD.
BMI, body mass index; RE, radiation enteritis; RTOG, Radiation Therapy Oncology Group; WMT, washed microbiota transplantation.

identified five species enriched in responders: *Bifidobacterium bifidum*, *Ruminococcus torques*, *Megamonas funiformis*, *Desulfovibrio piger* and *H. biformis* (linear discriminant analysis >4, figure 1J). Among these, only *H. biformis* showed a significant increase in relative abundance post-WMT ($p<0.05$, figure 1K). Heatmap analysis further revealed *H. biformis* as the sole strain positively correlated with responders and significantly enriched compared with non-responders ($p<0.05$, figure 1L).

We then assessed *H. biformis* abundance in healthy controls. Donors exhibited significantly higher levels of *H. biformis* than RE patients ($p<0.05$, figure 1M), with 14 of 15 RE patients lacking detectable levels pre-WMT. Following the detection of the candidate probiotic bacteria in our RE cohort, we sought to evaluate whether the abundance of *H. biformis* was consistent in other intestinal disorders. In the Human Intestinal Metagenome Database (GMrepo, https://gmrepo.humangut.info/home),[14] *H. biformis* was present in 30.1% (4894/16282) of the healthy population, vs 19.3% (117/605) in patients with inflammatory bowel disease (IBD) and 16.5% (52/377) with other intestinal diseases (online supplemental figure S3D,E, both $p<0.0001$). Overall, the abundance of *H. biformis* was significantly higher in healthy controls than in patients with intestinal diseases (online supplemental figure S3F, $p<0.05$). These findings suggest *H. biformis* as a key candidate for enhancing WMT efficacy, supported by its positive correlation with clinical response and higher detection rates in healthy populations.

Table 2 The details of patients with RE who received washed microbiota transplantation

Variables	Total (n=57)
Delivering route, n (%)	
Mid-gut	24 (42.11)
Colonic TET	33 (57.89)
Form of washed bacterial suspension, n (%)	
Fresh	29 (50.88)
Frozen	12 (21.05)
Both	16 (28.07)
Previous therapy, n (%)	
Antidiarrheic/painkiller/haemostatic drugs	52 (91.23)
Probiotic	29 (50.88)
Mesalazine	9 (15.79)
Corticosteroids	15 (26.32)
Clinical cure, n (%)	
Week 4	5 (8.77)
Week 8	12 (21.05)
Week 12	14 (24.56)
Adverse events, n (%)	3 (5.26)

RE, radiation enteritis; TET, transendoscopic enteral tubing.

Hb-auWMT outperforms WMT for treating RE model mice

Pursuing the idea that augmenting WMT with *H. biformis* may confer superior benefits over WMT in treating RE, we developed the concept of Hb-auWMT and experimentally evaluated its efficacy using the radiated mice model of RE.[15 16] After determining the optimal concentration of *H. biformis* for treating RE in vivo (online supplemental figure S4A–C), two separate experiments were designed to assess the changes in RE symptoms and survival rates under 13 Gy and 15 Gy doses of X-ray radiation, respectively (figure 2A,B). In the routine-dose radiation model, we observed an increasing trend in body weight in the Hb-auWMT group compared with the WMT group (figure 2C). In the high-dose radiation model, the Hb-auWMT group showed an 80% survival rate, whereas the WMT group showed a 60% survival rate (figure 2D).

Next, we wanted to determine if Hb-auWMT could significantly improve colitis compared with conventional WMT. In the routine-dose radiation model, we observed the typical colitis symptoms, including diarrhoea (wet tail) and haematochezia (faecal occult blood) in mice, with corresponding endoscopic characteristics (figure 2E). The Hb-auWMT group showed a significant decrease in DAI, diarrhoea and haematochezia compared with the WMT group (all $p<0.05$, figure 2F). Hb-auWMT also significantly mitigated the shortening of the colon length compared with WMT ($p<0.05$, figure 2G,H). Although we observed a significant increase in the spleen index in the Hb-auWMT group compared with the WMT group ($p<0.05$, figure 2I,J), the thymus index showed only an increasing trend in the Hb-auWMT group compared with the WMT group (figure 2I,J).

After Hb-auWMT demonstrated superior efficacy compared with WMT in treating RE symptoms in mice, we aimed to assess whether it could also exhibit superior anti-inflammatory effects. The histopathological sections showed that the intestinal mucosal structure in mice with radiation was severely damaged, characterised by neutrophil infiltration and extensive epithelial cell necrosis (figure 2K). Hb-auWMT had a stronger efficacy in restoring the integrity of colonic epithelium and decreasing cell necrosis (figure 2K), with a significant difference

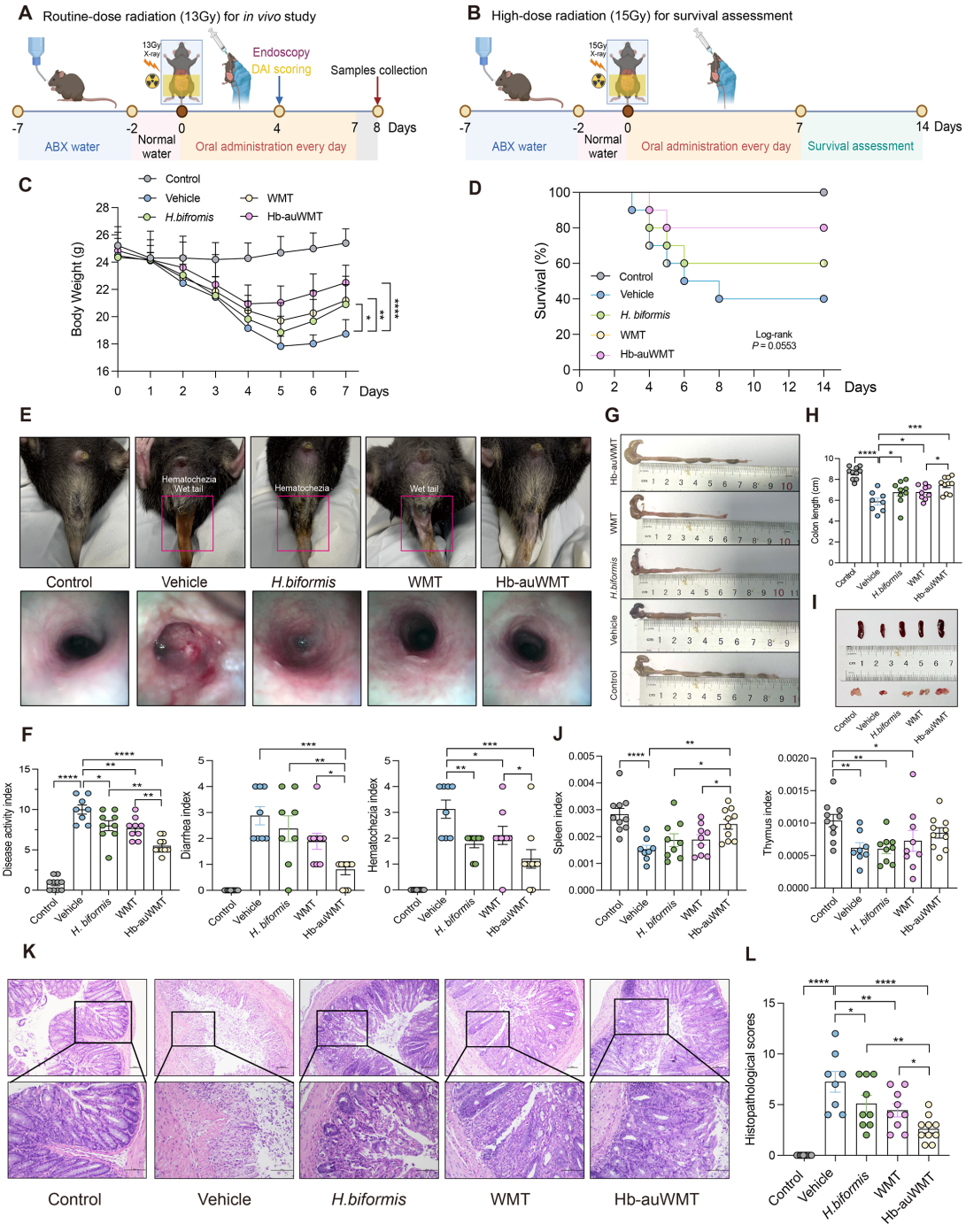

Figure 2 The anti-RE efficacy of Hb-auWMT outperforms WMT in mice models. (A) C57BL/6J mice were administered 5 days of antibiotic (ABX) water, which contained ampicillin (0.5 g/L), vancomycin (0.25 g/L), neomycin (0.5 g/L) and metronidazole (0.5 g/L). Following this, the mice were given normal water for 2 days. The routine-dose radiation used to assess the disease phenotype was 13 Gy X-rays. Body weights were recorded daily from day 0 to day 7, and other indicators were evaluated at the specified time points. (B) C57BL/6J mice were given the same pretreatment as the routine-dose radiation group. The high-dose radiation used to assess the survival rate was 15 Gy X-rays. Survival of C57BL/6J mice was evaluated daily from day 0 to day 14. (C) Changes in body weight were recorded in different groups of mice. The control group was not irradiated and received the vehicle solution by gavage (n=10). Other groups were irradiated. The vehicle group received the vehicle solution by gavage (n=8). The WMT and *Holdemanella biformis* groups received the WMT and *H. biformis* solution by gavage (n=9), respectively. The Hb-auWMT group received the *H. biformis* solution combined with the WMT solution by gavage (n=10). (D) The survival curve. (E) Representative photographs and endoscopic images of the diarrhoea and haematochezia on day 4. (F) Comparison of DAI scores, with the diarrhoea index and haematochezia index. (G) Representative photographs of excised colon tissues. (H) Comparison of the colon length. (I) Representative photographs of the excised spleen and thymus. (J) Comparison of the spleen and thymus index. (K) H&E staining images of the colon section. Scale bars, 100 µm. (L) Comparison of the histopathological scores. The n value in (F), (H), (J, L): control group n=10, vehicle group n=8, *H. biformis* group n=9, WMT group n=9, Hb-auWMT group n=10. The data were represented as mean±SD. The data in (C), (F), (H), (J, L) were analysed by one-way ANOVA test. The data in (D) were analysed by log-rank test. Two-tailed *p<0.05, **p<0.01, ***p<0.001, ****p<0.0001. ANOVA, analysis of variance; WMT, washed microbiota transplantation.

in histopathological scores compared with the WMT group ($p<0.05$, figure 2L). Collectively, these findings indicated that Hb-auWMT outperformed conventional WMT for treating RE model mice.

Hb-auWMT significantly alleviates the radiation-induced intestinal damage compared with WMT

Radiation directly induces enterocyte apoptosis, disrupting intestinal tight junctions and compromising the intestinal barrier.[17] We investigated whether Hb-auWMT could mitigate intestinal barrier damage more effectively than WMT. Immunofluorescence analysis of colonic tissues revealed significantly higher ZO-1 and Muc-2 expression in the Hb-auWMT group compared with the WMT group (figure 3A,C), while Occludin, E-cadherin and Claudin-3 showed only an increasing trend (figure 3A,C and online supplemental figure S4D,E). To assess alterations in mucus thickness, a critical component of intestinal barrier function, we performed AB-PAS staining on colonic tissues. The analysis revealed a significantly greater AB-PAS-positive area in the Hb-auWMT group compared with the WMT group (figure 3B,D), indicating enhanced mucus preservation. Since antiapoptosis and the proliferation of intestinal stem cells have functions to maintain intestinal barrier integrity,[18] we evaluated whether Hb-auWMT could more effectively reduce apoptosis or enhance the proliferation of enterocytes compared with WMT. Although apoptotic cells were significantly reduced in the Hb-auWMT group compared with the WMT group, Ki-67-positive cell counts did not differ significantly between the two groups (figure 3B, online supplemental figure S4F). These findings suggest that Hb-auWMT exerts stronger anti-apoptotic effects than WMT, thereby more effectively preserving intestinal barrier integrity.

Next, we aimed to determine whether Hb-auWMT could significantly reduce inflammatory cytokines. ELISA analysis showed that the expression levels of lipopolysaccharide, IL-1β, TNF-α and iNOS were significantly decreased in the Hb-auWMT group compared with the WMT group (figure 3E). Although no significant differences in IL-17 were observed between the two groups (figure 3E), the expression levels of IL-17 in the WMT group were nearly identical to those in the control group. This could account for why Hb-auWMT failed to further decrease these inflammatory cytokines. Using the qRT-PCR, we also observed that the relative expressions of IL-1β and iNOS decreased significantly in the Hb-auWMT group compared with the WMT group (figure 3F).

As epithelial hypoxia has a function in maintaining the integrity of the intestinal barrier,[19] we examined whether Hb-auWMT could enhance epithelial hypoxia more effectively than WMT. Using pimonidazole, an exogenous hypoxic marker, we visualised that the intensity of hypoxic macromolecules in the intestinal lumen of the Hb-auWMT group was significantly higher than in the WMT group ($p<0.05$, figure 3G,H). Collectively, Hb-auWMT demonstrated superior efficacy in mitigating radiation-induced intestinal barrier damage, suppressing inflammatory cytokines, enhancing antiapoptotic effects and maintaining epithelial hypoxia compared with WMT.

Hb-auWMT significantly increases Treg cell levels compared with WMT to modulate the imbalance between Treg and Th17 cells

The increase in Th17 cells and the decrease in Treg cells are characteristic of impaired intestinal immunity, which can exacerbate intestinal inflammation.[20 21] Although previous studies revealed that gut microbiota was essential in restoring radiation-impaired intestinal immunity,[22] evidence from clinical trials remains limited. We used flow cytometry on peripheral blood to determine if WMT could improve radiation-impaired immunity in 10 RE patients from the WMT group (online supplemental figure S5A). These patients showed a significant increase in Treg cell numbers after 7 days of WMT (online supplemental figure S5B). We also indirectly observed a decrease in Th17 cells, as evidenced by a significant reduction in IL-17 levels in RE patients after 7 days of WMT (online supplemental figure S5C). Since IL-17 is the principal secretion product of Th17 cells, an elevated level of IL-17 can reflect an increase in the number of Th17 cells and their enhanced activity.[23] These findings revealed the efficacy of WMT in increasing Treg cell levels and decreasing Th17 cell levels in RE patients, thus restoring impaired immunity.

Next, we wanted to determine whether Hb-auWMT could more effectively increase Treg cell levels and decrease Th17 cell levels in the RE mouse model compared with WMT (online supplemental figure S5A). Using mass cytometry, we characterised the relative abundance of these immune cells in the lamina propria of the colon (figure 4A). The relative abundance of these cell types was expressed as a percentage of overall $CD45^+$ T cells. The cDC cells were significantly increased in the Hb-auWMT group compared with the WMT group ($p<0.05$, figure 4B). Then we evaluated the percentage changes in Treg cells and Th17 cells (figure 4C). Although Hb-auWMT showed a significant increase in Treg cells compared with WMT (figure 4D), the Hb-auWMT group only exhibited a downward trend in Th17 cells compared with the WMT group (figure 4E). Collectively, these findings revealed that WMT could restore radiation-impaired immunity in RE patients and Hb-auWMT was more effective in increasing Treg cell levels than WMT.

Hb-auWMT restores radiation-induced gut microbiota dysbiosis

Gut microbiota dysbiosis frequently occurs in RE.[24] We performed 16S rRNA gene sequencing on faecal samples to characterise microbiota composition. The vehicle group showed a significant decrease in the α-diversity, using Shannon and Simpson index, compared with the control group (both $p<0.01$, online supplemental figure S6A,B), indicating gut microbiota dysbiosis. Hb-auWMT significantly mitigated the α-diversity reductions compared with the vehicle group (both $p<0.01$, online supplemental figure S6A,B). The β-diversity analysis demonstrated a distinct shift in bacterial composition towards that of the control group following Hb-auWMT treatment, suggesting a restorative effect on gut microbiota dysbiosis (online supplemental figure S6C). The microbiota composition across the groups at the phylum level was shown (online supplemental figure S6D). At the genus level, the Hb-auWMT group significantly increased the relative abundance of *Lachnospiraceae* compared with the vehicle group ($p<0.01$, online supplemental figure S6E). We also observed a significant increase in the *Limosilactobacillus* genus in the Hb-auWMT group compared with the WMT group ($p<0.01$, online supplemental figure S6F).

Hb-auWMT promotes the retention of *H. biformis* in the colon

Next, we wanted to investigate whether Hb-auWMT increased relative expressions of *H. biformis*, as it had functions to the clinical response after WMT treatment. The qRT-PCR analysis of faecal samples revealed that the relative expressions of *H. biformis* were significantly higher in the Hb-auWMT group than in the WMT group ($p<0.0001$, online supplemental

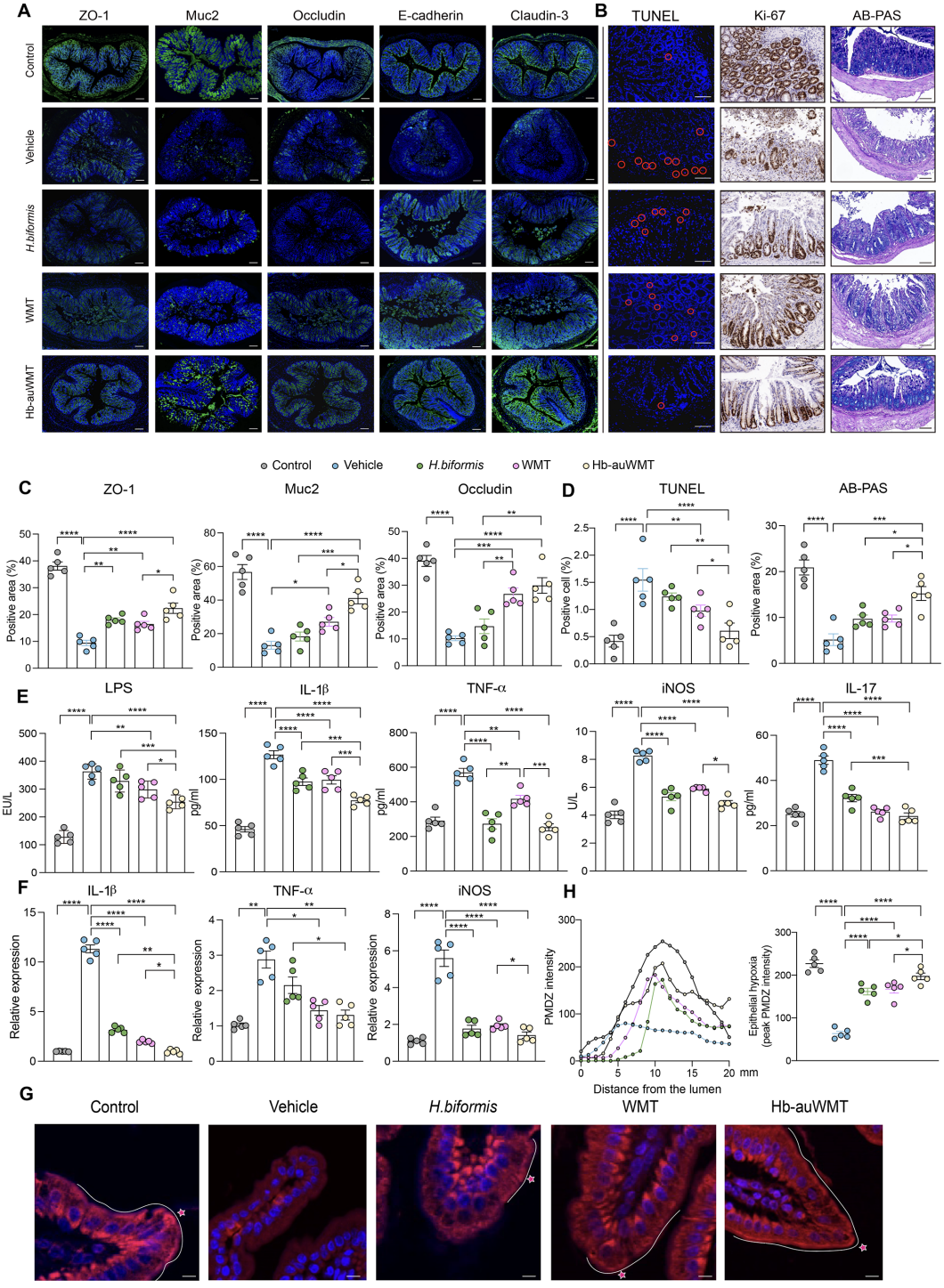

Figure 3 Hb-auWMT mitigates radiation-induced intestinal barrier injury and inflammation. (A) Representative fluorescence images showing the levels of tight junction protein ZO-1, Occludin Muc2, E-cadherin, and Claudin-3. Blue: DAPI$^+$ cells, green: protein of ZO-1, Occludin, Muc2, E-cadherin and Claudin-3. Scale bars, 100 µm. (B) Representative fluorescence and immunohistochemical images showing the levels of cell apoptosis and proliferation, and levels of mucins by TUNEL, Ki-67 and AB-PAS staining, respectively. For TUNEL staining, blue: DAPI$^+$ cells, red: TUNEL kit. For Ki-67 staining, blue: haematoxylin$^+$cells, brown: Ki-67$^+$ cells. For AB-PAS staining, blue: AB$^+$ acidic mucins, red: PAS$^+$ neutral mucins. Scale bars, 100 µm. (C) Expression of ZO-1, Occludin and Muc2 in colon tissues (n=5 in each group). (D) The positive cells of TUNEL and AB-PAS in colon tissues (n=5 in each group). (E) Relative protein expressions of pro-inflammatory cytokines (LPS, IL-1β, TNF-α, iNOS and IL-17) in colon tissues (n=5 in each group). (F) Relative mRNA expressions of pro-inflammatory cytokines IL-1β, TNF-α and iNOS in colon tissues (n=5 in each group). (G–H) Pimonidazole (PMDZ) reflects the degree of epithelial hypoxia. PMDZ was detected using a hypoxyprobe-1 primary antibody and a Cy-3 conjugated goat anti-mouse secondary antibody (red fluorescence) in colon sections counterstained with nuclear stain (blue fluorescence). Scale bars, 20 µm. (G) Representative images for each group after 7 days of treatment. The asterisk symbol indicates the location of the highest fluorescence intensity. (H) The PMDZ intensity from the lumen across the epithelial layer (distance in arbitrary units) and the average peak PMDZ intensity (n=5 in each group). The data were represented as mean±SEM. Data in (C–F, H) were analysed by one-way ANOVA test or the Kruskal-Wallis test. Two-tailed *p<0.05, **p<0.01, ***p<0.001, ****p<0.0001. ANOVA, analysis of variance; LPS, lipopolysaccharide.

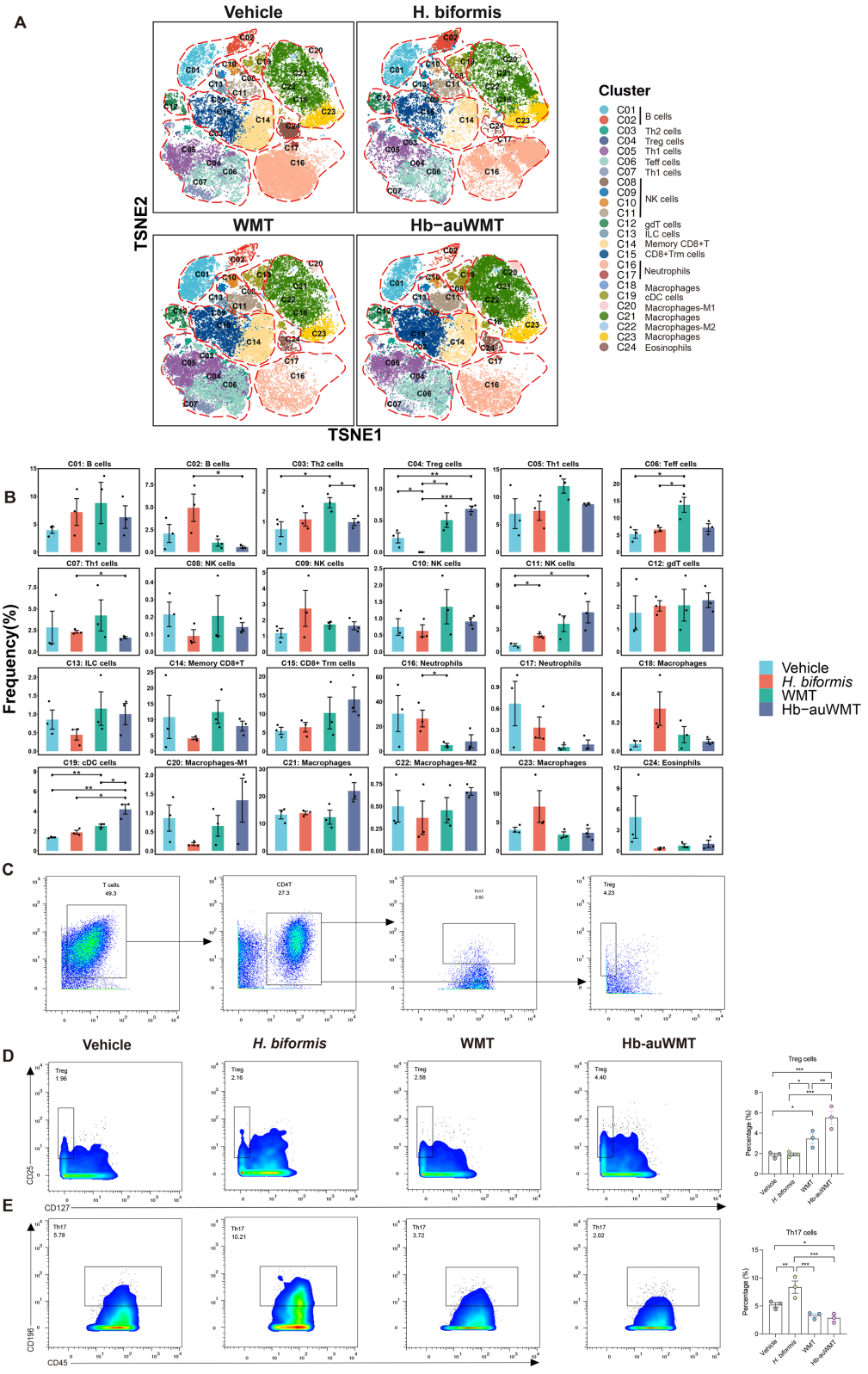

Figure 4 Hb-auWMT enhances Treg cell populations to modulate the imbalance between Treg and Th17 cells. (A) Mass cytometric analysis and mapping of colonic immune cells from mice with irradiated, *Holdemanella biformis*, WMT and Hb-auWMT (right) using CyTOF mass spectroscopy, t-distributed stochastic neighbour embedding (t-SNE) and clustering algorithms. (B) Comparisons of the percentages of major immune cell subsets of CD45$^+$ immune cells across groups (n=3 in each group). (C–E) Flow cytometry analysis demonstrating the differences in proportions of Th17 and Treg cells from colonic immune cells among mice with irradiated, *H. biformis*, WMT and Hb-auWMT. (C) Gating strategies for the Treg and Th17 cells. (D) Representative FACS plots and the histograms showing the percentage of CD4$^+$CD25$^+$CD127^{lo} (Treg) cells (gated on CD3$^+$ cells) (n=3 in each group). (E) Representative FACS plots and the histograms showing the percentage of CD3$^+$CD4$^+$CD196 (Th17) cells (n=3 in each group). Data in (B) were presented as mean±SD. Data in (D, E) were presented as mean±SEM. Comparisons were analysed by the unpaired Student's t-test. Two-tailed *p<0.05, **p<0.01, ***p<0.001. CyTOF, cytometry by time of flight; WMT, washed microbiota transplantation.

figure S6G). We then investigated whether Hb-auWMT could increase its retention in the intestine. We labelled *H. biformis* with FITC-D-Lysine and administered it to RE mice, then assessed fluorescence intensity at 24-hour and 72-hour intervals (online supplemental figure S6H). Fluorescence imaging of the colons revealed a significant increase in fluorescence intensity in the Hb-auWMT group compared with the *H. biformis* group ($p<0.05$, online supplemental figure S6I,J). We also designed a FISH probe specific to *H. biformis* to detect it in the intestine tissues. We observed consistent changes at 24 hours ($p<0.05$) and 72 hours ($p<0.001$, online supplemental figure S6K,L).

The conditioned medium from *H. biformis* augments the efficacy of WMT

To determine whether the augmentative function in Hb-auWMT was attributed to *H. biformis* itself or its metabolites, *H. biformis* conditioned medium (Hb.CM) was prepared via centrifugation and sterile filtration (online supplemental figure S7A), and compared with live *H. biformis* in RE mice, both combination with WMT. Hb.CM-auWMT showed similar improvements in body weight recovery after radiation (online supplemental figure S7B), DAI scores (online supplemental figure S7C), and mucosal integrity (online supplemental figure S7D,E) compared with Hb-auWMT. Inflammatory cytokine at mRNA or protein levels (IL-6, IL-1β, TNF-α and iNOS) did not show a difference between the Hb.CM-auWMT and Hb-auWMT (online supplemental figure S7F,G). These findings demonstrated that metabolites from *H. biformis* were essential to drive augmented therapeutic outcomes of Hb-auWMT.

Given the thousands of studies about butyric acid, and considering a report that *H. biformis* is a SCFA producer,[25] the targeted metabolomics analysis on SCFAs in the Hb.CM was performed. We observed significantly elevated levels of butyric and valeric acids in the Hb.CM compared with the uninoculated BHI medium control (both $p<0.001$, online supplemental figure S7H,I). This finding indicated that butyric and valeric acids were the essential metabolites of *H. biformis* augmenting the therapeutic effects of Hb-auWMT in RE.

Hb-auWMT significantly elevates the levels of butyric and valeric acids compared with WMT in treating RE

We performed targeted SCFA metabolomics on faecal samples from mice to investigate whether the apparent benefits of Hb-auWMT were attributable to increased levels of butyric acid and/or other SCFAs. The Hb-auWMT group had higher butyric and valeric acids compared with the WMT group (both $p<0.05$, figure 5A).

In previous studies involving animal experiments, it has been confirmed that valerate exhibits therapeutic efficacy against RE at an effective concentration of 0.3 mg/mL.[16] Given that the valeric acid concentrations in Hb-auWMT and Hb.CM are significantly lower than those of butyric acid, this may raise concerns regarding the therapeutic effectiveness of valeric acid in Hb-auWMT for RE. Therefore, we conducted experiments to verify whether adding 0.3 mg/mL valerate to drinking water could elevate faecal valeric acid levels to those comparable with the Hb-auWMT group. The results demonstrated that a valerate concentration of 0.3 mg/mL achieved the effective faecal valeric acid concentration observed in the Hb-auWMT group, confirming the feasibility of this concentration (online supplemental figure S8A).

To match the ratio of valeric acid and butyric acid concentrations in the faeces of the Hb-auWMT group, animal experiments were conducted using a low concentration of valeric acid (0.006 mg/mL). The results indicated that at this low concentration, the therapeutic effect on RE model mice was not significant (online supplemental figure S8B–D). Furthermore, the valeric acid content in the faeces of these mice was measured after 7 days, revealing an average concentration of 3155.85 ng/g, which was 10-fold lower than that of the Hb-auWMT group (online supplemental figure S8A). This suggests that the lower valeric acid concentration failed to reach the therapeutic threshold required for efficacy. Consequently, we proceeded with experiments using valeric acid at a concentration equivalent to that of butyric acid (0.3 mg/mL).

To determine if butyric and valeric acids had a direct function to the therapeutic efficacy. Butyrate and valerate were dissolved in water and provided to mice for continuous drinking over 7 days (figure 5B). Subsequently, the mice underwent abdominal radiation of 13 Gy and resumed drinking the supplemented water for 7 days (figure 5B). Both butyrate and valerate significantly mitigated the radiation-induced weight loss and the reduction of the colon length compared with the vehicle group (figure 5C–E).

We also observed a significant reduction in DAI scores in the butyrate group compared with the vehicle group (figure 5D,F). Using the histopathological scores, we observed that butyrate and valerate significantly mitigated colonic injury compared with the vehicle group (figure 5G,H). Next, we observed elevated levels of tight junction proteins ZO-1, Occludin and Muc2 (figure 5G,I) and reduced expression of IL-1β, TNF-α, IL-17 and iNOS in butyrate and valerate groups compared with the vehicle group (figure 5J and online supplemental figure S8E). The butyrate and valerate also elevated the levels of Treg cells while reducing the levels of Th17 cells (online supplemental figure S8F,G). Collectively, Hb-auWMT significantly increased butyrate and valerate levels compared with WMT, both of which had direct functions in treating RE.

Hb-auWMT mediates the therapeutic efficacy by upregulating the PPAR-γ pathway

Next, we wanted to determine the signal pathways having functions to the efficacy of Hb-auWMT. We performed RNA-Seq analysis to identify the genes regulated in the colonic tissue of mice receiving routine radiation doses. 70 genes were upregulated and 69 genes were downregulated in the Hb-auWMT group compared with the vehicle group (figure 6A). Pathway enrichment analysis revealed a significant difference in the peroxisome proliferator-activated receptor (PPAR) pathway in the Hb-auWMT group compared with the vehicle group ($p<0.05$, figure 6B). As PPAR has several subtypes (α, β/δ and γ), we used qRT-PCR to examine the corresponding relative mRNA expressions. The expression of PPAR-γ was significantly higher than other subtypes and increased significantly in the Hb-auWMT group than the vehicle group ($p<0.0001$, figure 6C). The subsequent western blot analysis also showed a consistent finding ($p<0.0001$, figure 6D,E).

We then investigated whether blocking PPAR-γ expression could reduce the efficacy of Hb-auWMT. We administered the PPAR-γ signalling antagonist GW9662 via daily peritoneal injections to the mice (figure 6F). The protective effects against weight loss, increased DAI scores and colon shortening in the Hb-auWMT plus GW9662 group were significantly reduced compared with the Hb-auWMT group (figure 6G–J). At the histological level, the damaged intestinal mucosal structure with neutrophil infiltration and extensive epithelial cell necrosis also did not recover (figure 6K). The ELISA and qRT-PCR

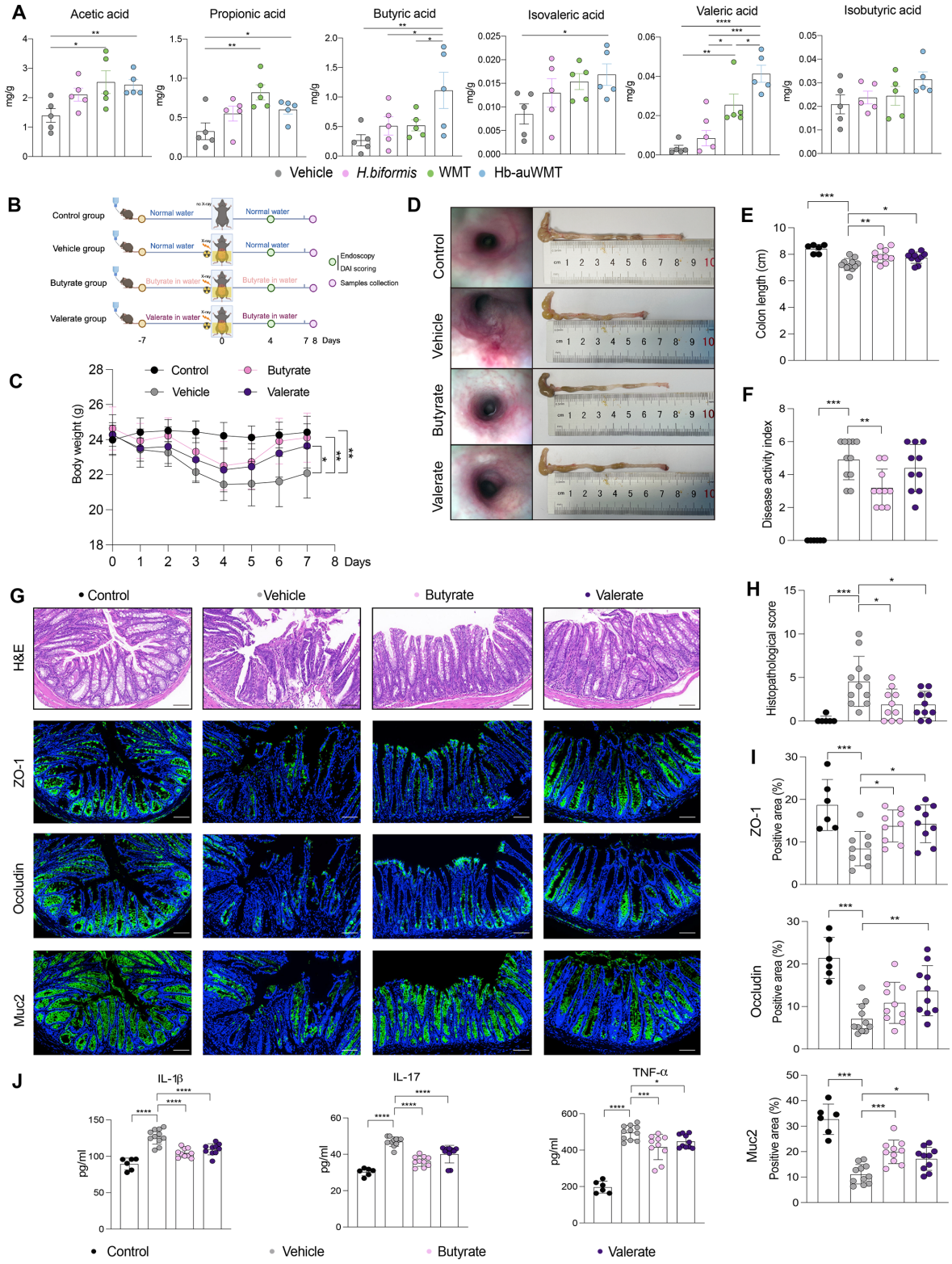

Figure 5 Butyric acid and valeric acid produced by Hb-auWMT alleviate radiation-induced intestinal injury. (A) The level of each SCFA in the faeces of mice among different groups (n=5/group). (B) Experimental schema of different groups. (C) Comparison of body weight across groups: control group (n=6), vehicle group (n=11), butyrate group (n=10) and valerate group (n=10). (D) Representative photographs and endoscopic images of excised colons. (E) Comparison of the colon length across groups. (F) Comparison of the DAI scores across groups. (G) Representative H&E staining and fluorescence images showing the expression of tight junction proteins ZO-1, Occludin and Muc2. Blue: DAPI+cells; green: ZO-1, Occludin or Muc2 proteins. Scale bars: 100 µm. (H) Comparison of the histopathological scores across groups. (I) Comparison of the expression of ZO-1, Occludin and Muc2 in the colon across groups. (J) Comparison of the expression of IL-1β, TNF-α and IL-17 in colon across groups by ELISA. The n value in (B), (C), (E), (F), (I, J): control group n=6, vehicle group n=11, butyrate group n=10, valerate group n=10. The data were represented as mean±SEM. All data were analysed by one-way ANOVA followed by Tukey's multiple-comparison tests or a two-tailed unpaired Student's t-test. Two-tailed *p<0.05, **p<0.01, ***p<0.001, ****p<0.0001. ANOVA, analysis of variance; SCFA, short-chain fatty acids; WMT, washed microbiota transplantation.

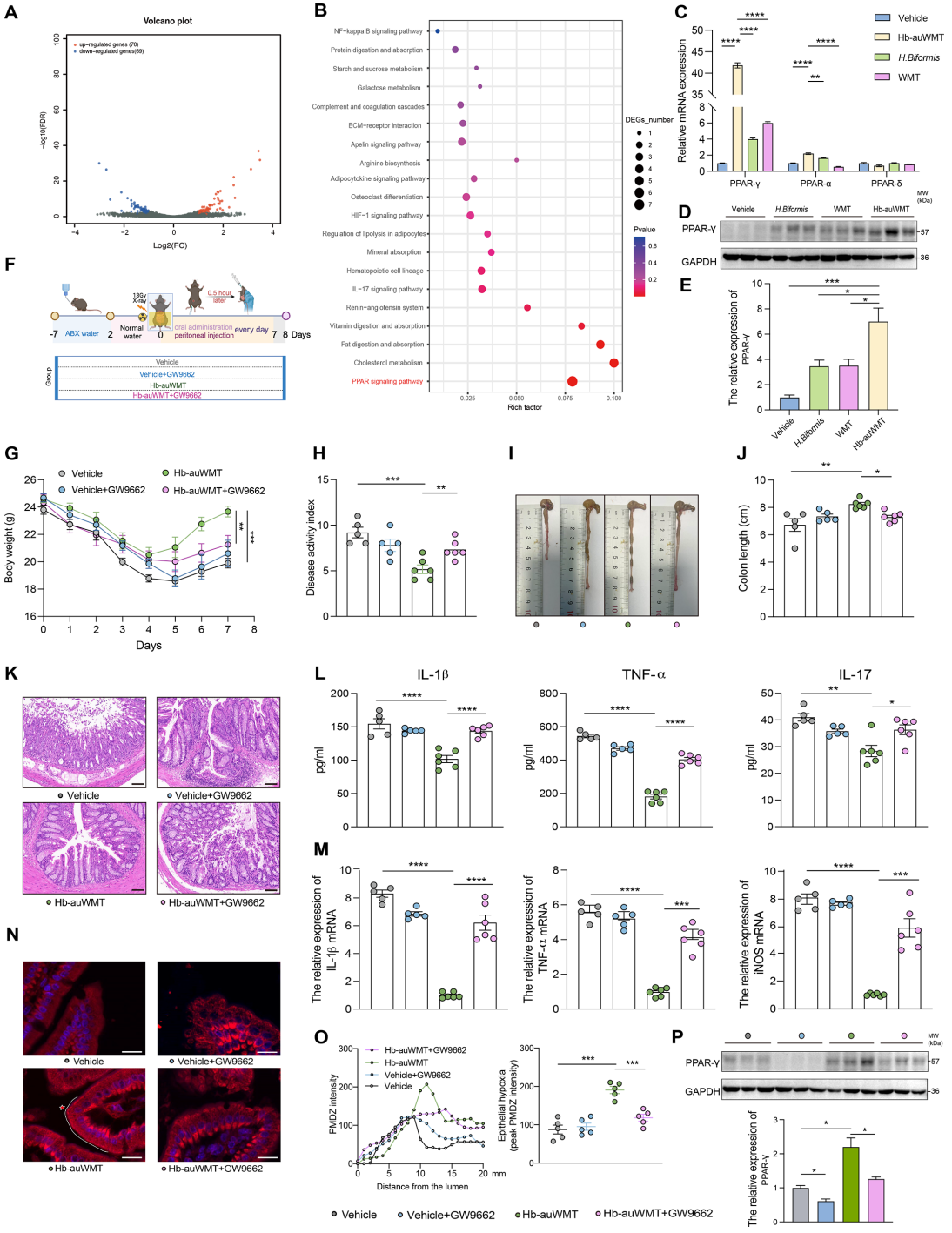

Figure 6 PPAR-γ upregulation mediates Hb-auWMT's anti-inflammatory effects. (A) Volcano plot of differentially expressed genes in the colon between the vehicle group and the Hb-auWMT group (n=4/group). (B) Analysis of differentially expressed signalling pathways in the colon between the vehicle group and the Hb-auWMT group (n=4/group). (C) Comparison of the relative mRNA expressions of PPAR-γ, PPAR-α and PPAR-δ in the colon across groups by qRT-PCR (n=5/group). (D) The relative expression of PPAR-γ in the colon across groups by western blot (n=3/group). (E) Comparison of the relative protein expressions of PPAR-γ in the colon across groups by western blot (n=3/group). (F) Experimental schema of different groups. (G) Comparison of body weight across groups: vehicle group (n=5), vehicle+GW9662 group (n=5), Hb-auWMT group (n=6), Hb-auWMT+GW9662 group (n=6). (H) Comparison of the DAI scores across groups. (I) Representative photographs of excised colons. (J) Comparison of the colon length across groups. (K) Representative H&E staining images of the colon section. Scale bars, 100 μm. (L) Comparison of the protein levels of IL-1β, TNF-α and IL-17 in the colon by ELISA. (M) Comparison of the relative mRNA expressions of IL-1β, TNF-α and iNOS in the colon by qRT-PCR. (N) Representative images of epithelial hypoxia for each group after 7 days of treatment. The asterisk symbol indicates the location of the highest fluorescence intensity. (O) The PMDZ intensity from the lumen across the epithelial layer (distance in arbitrary units), and the comparison of average peak PMDZ intensity (n=5/group). (P) Comparison of the relative protein expressions of PPAR-γ in the colon across groups by western blot (n=3/group). The n value in (G), (H), (J), (L, M): vehicle group n=5, vehicle+GW9662 group n=5, Hb-auWMT group n=6. The data were represented as mean±SEM. Data were analysed by one-way ANOVA followed by Tukey's multiple-comparison tests or a two-tailed and unpaired Student's t-test. Two-tailed *p<0.05, **p<0.01, ***p<0.001, ****p<0.0001. ANOVA, analysis of variance; WMT, washed microbiota transplantation.

experiments showed that the reduction of IL-1β, TNF-α, IL-17 and iNOS levels was significantly suppressed in the Hb-auWMT group after blocking PPAR-γ ($p<0.05$, figure 6L,M). We also observed that Hb-auWMT failed to recover in the hypoxic environment of the radiated intestinal lumen following PPAR-γ blockade (figure 6N,O). Western blot analysis confirmed that PPAR-γ was effectively inhibited by GW9662 ($p<0.05$, figure 6P). Collectively, PPAR-γ is an essential signal pathway for the therapeutic efficacy of Hb-auWMT.

DISCUSSION

Previous studies have linked gut microbiota dysbiosis to the onset and progression of RE,[26 27] yet the clinical evidence for microbiota reconstruction in treating RE remains limited.[28] FMT from irradiated mice increased inflammatory cytokines in germ-free models,[29] while FMT from healthy mice reduced inflammation, improvedsymptoms, and enhanced survival rates in irradiated mice.[30] Our cohort showed WMT effectively treated RE, achieving a 70.6% response rate (25.5% clinical cure) within 12 weeks, outperforming routine treatments. RE is a condition with various symptoms or combinations of symptoms.[31] WMT addresses multiple RE symptoms, though efficacy declined between weeks 8 and 12, suggesting repeated courses may be necessary. This will be clarified by our ongoing long-term study.

We identified *H. biformis* as a key microbe enriched in responders, absent in 93.3% of pretreatment RE patients. This aligns with findings linking *Holdemanella* abundance to favourable outcomes in inflammatory bowel disease and immune checkpoint inhibitor-associated colitis.[32 33] *H. biformis*, a producer of anti-inflammatory metabolites like SCFAs and 3-hydroxy octadecenoic acid,[34 35] aligns with findings linking *Holdemanella* to favourable outcomes in inflammatory diseases.[32 33 36] *H. biformis* has homology to *Faecalibaculum rodentium* and can suppress tumour proliferation.[25] These studies demonstrate the probiotic potential of *H. biformis*, supporting its selection as a candidate microbe for X-auWMT treatment.

Hb-auWMT outperformed WMT in the RE mice, enhancing survival and increasing beneficial bacteria like *Lachnospiraceae*, which is closely associated with restored haematopoiesis and gastrointestinal function.[37] *H. biformis* likely interacts with beneficial bacterial communities in WMT (eg, *Lachnospiraceae*, *Akkermansia* and *Turicibacter*), thereby enhancing WMT efficacy. However, single-strain probiotics face translational challenges due to low strain richness and limited colonisation, as observed with *H. biformis* in mice.[3 25 38] Hb-auWMT addresses this by providing a rich microbial ecosystem and an anaerobic colonic microenvironment for *H. biformis* survival.

PPAR-γ emerged as a central mediator of Hb-auWMT's effects, upregulating mucosal barrier proteins and attenuating RE. Its inhibition abolished these benefits.[39 40] Hb-auWMT restored colonic epithelial hypoxia, suppressing oxygen-tolerant pathogens (eg, *Enterobacteriaceae*) while supporting anaerobic bacteria.[41–43] Butyrate and valerate further contributed by enhancing epithelial integrity and rebalancing Treg/Th17 cells,[16 44 45] highlighting microbial regulation of the PPAR-γ pathway against colitis. Although PPAR-γ is primarily considered activatable by SCFAs, particularly butyrate,[44] synthetic bile acids can activate PPAR-γ.[46] The bile acid metabolism plays a crucial role in gut microbiota.[47] For instance, the secondary bile acid 3-succinylated cholic acid derived from *Bacteroides uniformis* has been demonstrated to promote the growth of *Akkermansia muciniphila* and alleviate metabolic dysfunction-associated steatohepatitis (MASH).[48] As a key receptor mediating the effects of gut microbial metabolites, PPAR-α is typically associated with bile acid metabolism. Inhibiting PPAR-α facilitates the production of hydrophilic bile acids and ameliorates MASH.[49] These findings suggest the potential for investigating the anti-inflammatory mechanisms of RE through the microbiota-bile acid pathway in the future.

This study has several limitations. First, Hb-auWMT requires confirmation in randomised controlled trials (RCTs) to establish causality. Second, whether *H. biformis* can be developed as a probiotic in the future for clinical applications requires further research. Third, longer follow-up and RCTs may uncover additional candidate strains and elucidate their roles in microbiota-host crosstalk.

In conclusion, WMT is a safe and effective therapeutic option for RE. Hb-auWMT has better efficacy in treating RE in mice compared with WMT. This study approves X-auWMT as a better microbiome-based therapeutic compared with specific probiotics and WMT, challenging the typical recognition of probiotics and microbiota transplantation.

Acknowledgements The authors would like to express their sincere gratitude to Jie Zhang, Yaoyao Chen and Lixia Xiong for providing data from the China Microbiota Transplantation System (www.fmtbank.org), Qianqian Li for providing guidance on study design, Xiaoshuang Xu for offering professional statistical guidance, Zheshun Pi and Keting Huang for providing assistance with animal experiments and Dengke Yao and Jiazhi Ye for collecting the clinical data.

Contributors Conceptualisation: WW and FZ; methodology: WW, QW, BC and FZ; clinical data acquisition: WW, YW, CLi and BY; bacterial experiment: WW and RW; in vitro experiment: WW, YY, RW and CLi; in vivo experiment: WW, XD, RW, CLu, CLi, GL and YY; visualisation: WW and SZ; radiation support and guidance: LZ; statistical guidance: JB; writing-original draft: WW and YY; writing-review and editing: PL, XD, BC and FZ; supervision: QW, BC and FZ. All authors reviewed and approved the final version of the manuscript. FZ is the guarantor.

Funding This work was supported by the National Natural Science Foundation of China (82170563), the National Key Research and Development Program of China (2021YFA0717004) and Nanjing Medical University Fan Daiming Research Funds for Holistic Integrative Medicine (2023-3HIM). All authors declare that the research was conducted in the absence of any commercial or financial relationships that could be construed as a potential conflict of interest.

Disclaimer The funding organisation, Nanjing Medical University, had no involvement in the study's design, execution, interpretation or writing, thereby ensuring the objectivity and integrity of our research findings were uncompromised.

Competing interests FZ conceived the concept of GenFMTer and TET and the devices (FMT Medical, Nanjing, China) related to them.

Patient and public involvement Patients and/or the public were not involved in the design, or conduct, or reporting, or dissemination plans of this research.

Patient consent for publication Consent obtained directly from patient(s).

Ethics approval This study involves human participants and was approved by the Institutional Ethical Review Board (2017-IIT-001-LP-01). Participants gave informed consent to participate in the study before taking part. The protocol of animal experiments was approved by the Ethics Committee of Nanjing Medical University Laboratory Animal Center (No. IACUC-2304042).

Provenance and peer review Not commissioned; externally peer reviewed.

Data availability statement Data are available on reasonable request. Data are available in the manuscript from the corresponding authors on reasonable request. The sequencing datasets in this study have been submitted in NCBI SRA with accession numbers PRJNA1207712.

ORCID iDs
Xiao Ding https://orcid.org/0000-0001-9068-8870
Faming Zhang https://orcid.org/0000-0003-4157-1144

REFERENCES

1 Sorbara MT, Pamer EG. Microbiome-based therapeutics. *Nat Rev Microbiol* 2022;20:365–80.
2 Wang Y, Zhang S, Borody TJ, *et al*. Encyclopedia of fecal microbiota transplantation: a review of effectiveness in the treatment of 85 diseases. *Chin Med J* 2022;135:1927–39.
3 Chen-Liaw A, Aggarwala V, Mogno I, *et al*. Gut microbiota strain richness is species specific and affects engraftment. *Nature New Biol* 2025;637:422–9.
4 Fecal Microbiota Transplantation-Standardization Study Group. Nanjing consensus on methodology of washed microbiota transplantation. *Chin Med J* 2020.
5 Zhang T, Lu G, Zhao Z, *et al*. Washed microbiota transplantation vs. manual fecal microbiota transplantation: clinical findings, animal studies and in vitro screening. *Protein Cell* 2020;11:251–66.
6 Perrucci E, Macchia G, Cerrotta A, *et al*. Prevention and management of radiotherapy-related toxicities in gynecological malignancies. *Position Paper on Behalf of AIRO (Italian Association of Radiotherapy and Clinical Oncology)* 2024;129:1329–51.
7 Peterson DE, Koyfman SA, Yarom N, *et al*. Prevention and Management of Osteoradionecrosis in Patients With Head and Neck Cancer Treated With Radiation Therapy: ISOO-MASCC-ASCO Guideline. *J Clin Oncol* 2024;42:1975–96.
8 Wang W, Cui B, Nie Y, *et al*. Radiation injury and gut microbiota-based treatment. *Protein Cell* 2024;15:83–97.
9 Glover M, Smerdon GR, Andreyev HJ, *et al*. Hyperbaric oxygen for patients with chronic bowel dysfunction after pelvic radiotherapy (HOT2): a randomised, double-blind, sham-controlled phase 3 trial. *Lancet Oncol* 2016;17:224–33.
10 Zhu J, Li X, Huang M, *et al*. Application of Recombinant Human Superoxide Dismutase in Radical Concurrent Chemoradiotherapy for Cervical Cancer to Prevent and Treat Radiation-induced Acute Rectal Injury: A Multicenter, Randomized, Open-label, Prospective Trial. *Int J Radiat Oncol Biol Phys* 2024;120:720–9.
11 Ding X, Li Q, Li P, *et al*. Fecal microbiota transplantation: A promising treatment for radiation enteritis? *Radiother Oncol* 2020;143:12–8.
12 Cox JD, Stetz J, Pajak TF. Toxicity criteria of the Radiation Therapy Oncology Group (RTOG) and the European Organization for Research and Treatment of Cancer (EORTC). *Int J Radiat Oncol Biol Phys* 1995;31:1341–6.
13 Marcella C, Cui B, Kelly CR, *et al*. Systematic review: the global incidence of faecal microbiota transplantation-related adverse events from 2000 to 2020. *Aliment Pharmacol Ther* 2021;53:33–42.
14 Wu S, Sun C, Li Y, *et al*. GMrepo: a database of curated and consistently annotated human gut metagenomes. *Nucleic Acids Res* 2020;48:D545–53.
15 Feng Y, Luo X, Li Z, *et al*. A ferroptosis-targeting ceria anchored halloysite as orally drug delivery system for radiation colitis therapy. *Nat Commun* 2023;14:5083.
16 Li Y, Dong J, Xiao H, *et al*. Gut commensal derived-valeric acid protects against radiation injuries. *Gut Microbes* 2020;11:789–806.
17 Li H, Zhao S, Jiang M, *et al*. Biomodified Extracellular Vesicles Remodel the Intestinal Microenvironment to Overcome Radiation Enteritis. *ACS Nano* 2023;17:14079–98.
18 Xie L-W, Cai S, Lu H-Y, *et al*. Microbiota-derived I3A protects the intestine against radiation injury by activating AhR/IL-10/Wnt signaling and enhancing the abundance of probiotics. *Gut Microbes* 2024;16:2347722.
19 Glover LE, Lee JS, Colgan SP. Oxygen metabolism and barrier regulation in the intestinal mucosa. *J Clin Invest* 2016;126:3680–8.
20 Geremia A, Biancheri P, Allan P, *et al*. Innate and adaptive immunity in inflammatory bowel disease. *Autoimmun Rev* 2014;13:3–10.
21 Ueno A, Jeffery L, Kobayashi T, *et al*. Th17 plasticity and its relevance to inflammatory bowel disease. *J Autoimmun* 2018;87:38–49.
22 Zhang L-L, Xu J-Y, Xing Y, *et al*. Lactobacillus rhamnosus GG alleviates radiation-induced intestinal injury by modulating intestinal immunity and remodeling gut microbiota. *Microbiol Res* 2024;286:127821.
23 Shao L, Li M, Zhang B, *et al*. Bacterial dysbiosis incites Th17 cell revolt in irradiated gut. *Biomed Pharmacother* 2020;131:110674.
24 He K-Y, Lei X-Y, Wu D-H, *et al*. *Akkermansia muciniphila* protects the intestine from irradiation-induced injury by secretion of propionic acid. *Gut Microbes* 2023;15:2293312.
25 Zagato E, Pozzi C, Bertocchi A, *et al*. Endogenous murine microbiota member Faecalibaculum rodentium and its human homologue protect from intestinal tumour growth. *Nat Microbiol* 2020;5:511–24.
26 Moraitis I, Guiu J, Rubert J. Gut microbiota controlling radiation-induced enteritis and intestinal regeneration. *Trends Endocrinol Metab* 2023;34:489–501.
27 Wang Z, Wang Q, Wang X, *et al*. Gut microbial dysbiosis is associated with development and progression of radiation enteritis during pelvic radiotherapy. *J Cellular Molecular Medi* 2019;23:3747–56.
28 Reis Ferreira M, Andreyev HJN, Mohammed K, *et al*. Microbiota- and Radiotherapy-Induced Gastrointestinal Side-Effects (MARS) Study: A Large Pilot Study of the Microbiome in Acute and Late-Radiation Enteropathy. *Clin Cancer Res* 2019;25:6487–500.
29 Gerassy-Vainberg S, Blatt A, Danin-Poleg Y, *et al*. Radiation induces proinflammatory dysbiosis: transmission of inflammatory susceptibility by host cytokine induction. *Gut* 2018;67:97–107.
30 Xiao H-W, Cui M, Li Y, *et al*. Gut microbiota-derived indole 3-propionic acid protects against radiation toxicity via retaining acyl-CoA-binding protein. *Microbiome* 2020;8:69.
31 van de Wetering FT, Verleye L, Andreyev HJN, *et al*. Non-surgical interventions for late rectal problems (proctopathy) of radiotherapy in people who have received radiotherapy to the pelvis. *Cochrane Database Syst Rev* 2016;4:CD003455.
32 Halsey TM, Thomas AS, Hayase T, *et al*. Microbiome alteration via fecal microbiota transplantation is effective for refractory immune checkpoint inhibitor-induced colitis. *Sci Transl Med* 2023;15:eabq4006.
33 Li Q, Ding X, Liu K, *et al*. Fecal Microbiota Transplantation for Ulcerative Colitis: The Optimum Timing and Gut Microbiota as Predictors for Long-Term Clinical Outcomes. *Clin Transl Gastroenterol* 2020;11:e00224.
34 Zhao L-Y, Mei J-X, Yu G, *et al*. Role of the gut microbiota in anticancer therapy: from molecular mechanisms to clinical applications. *Signal Transduct Target Ther* 2023;8:201.
35 Pujo J, Petitfils C, Le Faouder P, *et al*. Bacteria-derived long chain fatty acid exhibits anti-inflammatory properties in colitis. *Gut* 2021;70:1088–97.
36 Romaní-Pérez M, López-Almela I, Bullich-Vilarrubias C, *et al*. Holdemanella biformis improves glucose tolerance and regulates GLP-1 signaling in obese mice. *FASEB J* 2021;35:e21734.
37 Guo H, Chou W-C, Lai Y, *et al*. Multi-omics analyses of radiation survivors identify radioprotective microbes and metabolites. *Science* 2020;370:eaay9097.
38 Doron S, Snydman DR. Risk and safety of probiotics. *Clin Infect Dis* 2015;60 Suppl 2:S129–34.
39 Li D, Feng Y, Tian M, *et al*. Gut microbiota-derived inosine from dietary barley leaf supplementation attenuates colitis through PPARγ signaling activation. *Microbiome* 2021;9:83.
40 Bouguen G, Langlois A, Djouina M, *et al*. Intestinal steroidogenesis controls PPARγ expression in the colon and is impaired during ulcerative colitis. *Gut* 2015;64:901–10.
41 Zeng N, Wu F, Lu J, *et al*. High-fat diet impairs gut barrier through intestinal microbiota-derived reactive oxygen species. *Sci China Life Sci* 2024;67:879–91.
42 Sorbara MT, Littmann ER, Fontana E, *et al*. Functional and Genomic Variation between Human-Derived Isolates of Lachnospiraceae Reveals Inter- and Intra-Species Diversity. *Cell Host Microbe* 2020;28:134–46.
43 Lee J-Y, Tiffany CR, Mahan SP, *et al*. High fat intake sustains sorbitol intolerance after antibiotic-mediated Clostridia depletion from the gut microbiota. *Cell* 2024;187:1191–205.
44 Byndloss MX, Olsan EE, Rivera-Chávez F, *et al*. Microbiota-activated PPAR-γ signaling inhibits dysbiotic Enterobacteriaceae expansion. *Science* 2017;357:570–5.
45 He N, Chen K, Yu S, *et al*. Stachyose Exerts Anticolitis Efficacy by Re-balancing Treg/Th17 and Activating the Butyrate-Derived PPARγ Signaling Pathway. *J Agric Food Chem* 2024;72:12171–83.
46 Grander C, Meyer M, Steinacher D, *et al*. 24-Norursodeoxycholic acid ameliorates experimental alcohol-related liver disease and activates hepatic PPARγ. *JHEP Rep* 2023;5:100872.
47 de Vos WM, Tilg H, Van Hul M, *et al*. Gut microbiome and health: mechanistic insights. *Gut* 2022;71:1020–32.
48 Nie Q, Luo X, Wang K, *et al*. Gut symbionts alleviate MASH through a secondary bile acid biosynthetic pathway. *Cell* 2024;187:2717–34.
49 Dixon ED, Claudel T, Nardo AD, *et al*. Inhibition of ATGL alleviates MASH via impaired PPARα signalling that favours hydrophilic bile acid composition in mice. *J Hepatol* 2025;82:658–75.